INTERNATIONAL JOURNAL FOR NUMERICAL METHODS IN FLUIDS, VOL. 6, 841–853 (1986)

THE EFFECT OF THE STABILITY OF MIXED FINITE ELEMENT APPROXIMATIONS ON THE ACCURACY AND RATE OF CONVERGENCE OF SOLUTION WHEN SOLVING INCOMPRESSIBLE FLOW PROBLEMS

D. J. SILVESTER AND R. W. THATCHER

Department of Mathematics, University of Manchester Institute of Science and Technology, P.O. Box 88, Manchester M60 1QD, England

SUMMARY

The stability of two different mixed finite element methods for incompressible flow problems are theoretically analysed. The effect of the stability of the mixed approximation on the accuracy and the rate of convergence of solution is assessed for two non-trivial problems. The numerical results presented indicate that if the stability of the mixed approximation is not guaranteed then both pressure and velocity solutions are markedly less accurate. In one of the cases considered the ultimate convergence of both the pressure and the velocity solutions is seriously in doubt.

KEY WORDS Incompressible Flow Finite Element Stability Accuracy Convergence

INTRODUCTION

It is a well established fact that in order to be certain of success when solving incompressible flow problems using primitive variable formulations, the component mixed finite element approximations of velocity and pressure must be compatible. Theoretically, if a stability inequality of the form introduced by Babüska,[1] or Brezzi[2] is satisfied then the compatibility of the mixed approximation is guaranteed. A number of popular mixed FE methods for incompressible flow problems can be proved to give stable mixed approximations for all possible element subdivisions; several such methods are reviewed by Thomsset[3] and Fortin.[4]

A variety of elements for solving incompressible flow problems which are not stable in the classical sense are also in common use; for example, mixed and penalty finite element methods which exhibit spurious pressure modes are discussed by Sani *et al.*,[5] Engelman *et al.*[6] and Oden and Jacquotte.[7] Although error estimates and convergence proofs for regular grids of rectangular elements have been established, e.g. by Johnson and Pitkäranta[8] and by Malkus and Olsen,[9] the numerical results in References 5–7 indicate that these methods can be significantly less accurate than methods with guaranteed stability, particularly in the presence of 'impure' pressure modes.

In this paper the effect of the stability of the mixed approximation on the accuracy and rate of convergence of solution is assessed. In the first part of the paper, two simple triangular elements are analysed from the point of view of stability. One of the elements is shown to give stable mixed approximations for any element subdivision; the other is shown to be semi-stable in the sense that for a grid of rectangles all subdivided into two triangles the stability of the resulting mixed approximation depends on the triangulation strategy that is used in generating the grid.

0271–2091/86/110841–13$06.50
© 1986 by John Wiley & Sons, Ltd.
Received 18 January 1986
Revised 24 April 1986

In the second part of the paper, numerical results for these two elements are presented. The results illustrate that if the stability of the mixed approximation is guaranteed then optimal convergence rates of both the pressure and the velocity solutions can be measured. However, if stability is not guaranteed then the resulting solutions are not only significantly less accurate, the ultimate convergence of the pressure and the velocity can *both* be in doubt.

The primary intention of the paper is to illustrate the dangers that exist if flow problems of engineering importance are solved using elements which do not have stability guaranteed.

STABILITY THEORY

The general theory of the stability of mixed finite element methods is relevant to a number of incompressible flow formulations. The simplest formulation is the stationary Stokes equations in (two-dimensional) Cartesian co-ordinates

$$\begin{aligned} -\nabla p + \frac{1}{Re}\nabla^2 \mathbf{u} &= \mathbf{0}, \qquad \text{in } \Omega, \\ \operatorname{div} \mathbf{u} &= 0, \qquad \text{in } \Omega, \end{aligned} \tag{1}$$

with appropriate conditions on the boundary $\partial\Omega$ of the domain Ω. The classical weak formulation of the above problem is as follows: given appropriate velocity and pressure spaces V and Q, respectively, find $(\mathbf{u}, p) \in V \times Q$ such that

$$\begin{aligned} \frac{1}{Re}(\nabla \mathbf{u}, \nabla \mathbf{v}) - (\operatorname{div} \mathbf{v}, p) &= \mathbf{0}, \\ (\operatorname{div} \mathbf{u}, q) &= 0, \end{aligned} \tag{2}$$

for all $\mathbf{v} \in V$ and $q \in Q$, where $(.,.)$ is the usual inner product

$$(\mathbf{u}, \mathbf{v}) = \int\int_{\Omega} u_x v_x + u_y v_y \, \mathrm{d}x\mathrm{d}y. \tag{3}$$

The weak formulation can be discretized by introducing finite dimensional subspaces V^h and Q^h, to give the corresponding approximate problem: find $(\mathbf{u}^h, p^h) \in V^h \times Q^h$ such that

$$\begin{aligned} \frac{1}{Re}(\nabla \mathbf{u}^h, \nabla \mathbf{v}^h) - (\operatorname{div} \mathbf{v}^h, p^h) &= \mathbf{0}, \\ (\operatorname{div} \mathbf{u}^h, q^h) &= 0, \end{aligned} \tag{4}$$

for all $\mathbf{v}^h \in V^h$ and $q^h \in Q^h$.

In a finite element framework the spaces V^h and Q^h are characterized by the element subdivision T_h, and the polynomial approximations within the element. Three standard types of element approximation are of interest in this paper:

- Q_c: the quadratic polynomial defined by the three vertex node values and the three mid-side node values
- L_c: the linear polynomial defined by the three vertex node values
- L_d: the linear polynomial defined by the three mid-side node values.

It is assumed at the outset that the triangulation T_h is regular in the sense that the ratio of the diameters of the escribed and inscribed circles is bounded both above and below by constants which are independent of h, for every element in the triangulation. Applying the general theory of

mixed finite element methods, the stability of the mixed approximation $V^h \times Q^h$ is guaranteed if a Babüska–Brezzi type condition is satisfied, i.e. if a strictly positive constant c and be found such that

$$\sup_{\substack{\mathbf{v}^h \in V^h \\ \mathbf{v}^h \neq \mathbf{0}}} \frac{(\operatorname{div} \mathbf{v}^h, q^h)}{\|\mathbf{v}^h\|} \geqslant c \|q^h\| \tag{5}$$

for some norms compatible with V^h and Q^h, and for all $q^h \in Q^h$. If it can be shown that (5) is satisfied for some particular velocity/pressure polynomial approximation independently of the triangulation T_h then the element is said to be *uniformly* stable. Uniformly stable elements can always be used with confidence, for example in the knowledge that spurious pressure modes are not possible on any grid. Several such elements have been identified, for example by Crouzeix and Raviart,[10] but the most relevant example here corresponds to the mixed approximation

$$V^h = \{(v_x^h, v_y^h): v_x^h|_{\Delta_k} = Q_c, v_y^h|_{\Delta_k} = Q_c \text{ for all } \Delta_k \in T_h\},$$
$$Q^h = \{q^h: q^h|_{\Delta_k} = L_c \text{ for all } \Delta_k \in T_h\},$$

i.e. continuous quadratic approximation of the two components of velocity, with continuous linear approximation of the pressure over the same grid of triangular elements. The uniform stability of this element has been established by Bercovier and Pironneau.[11]

If the velocity/pressure polynomial approximation within an element is such that the element can exhibit spurious pressure modes then the element clearly cannot be uniformly stable. However, it is still possible to guarantee the stability of certain mixed approximations using such elements, for example by ensuring that the subdivision T_h satisfies additional geometric constraints. The key to establishing stability in these cases is to use local stability theory, a technique suggested by Stenberg.[12] The heart of the stability theory developed in Reference 12 is the so called 'macroelement condition'; here, any patch of elements which satisfies this fundamental condition is said to be *locally* stable.

Assuming that quadratic approximation is used for all components of velocity, a simple way of interpreting the macroelement condition is to consider an arbitrary velocity field with boundary data specified everywhere on the boundary of the patch; local stability then requires that the pressure field over the patch must be free of all spurious pressure modes. Expressed mathematically, if there are n velocity nodes strictly inside the patch, and a total of m pressure nodes inside and on the boundary of the patch, so that the local approximations are of the form

$$u_x^1 = \sum_{i=1}^{n} u_x^i N^i(x, y), \tag{6}$$

$$u_y^1 = \sum_{i=1}^{n} u_y^i N^i(x, y), \tag{7}$$

$$p^1 = \sum_{j=1}^{m} p^j M^j(x, y), \tag{8}$$

where $N^i(x, y)$ and $M^j(x, y)$ are the usual Lagrangian basis functions, then there exists a $(2n \times m)$ patch pressure matrix $\mathbf{C}^1$ which can be written in the form

$$\mathbf{C}^1 = \left[\frac{\mathbf{C}_x^1}{\mathbf{C}_y^1}\right], \tag{9}$$

with

$$\mathbf{C}_x^1(i,j) = \int\int_{\Omega^1} \frac{\partial N_i}{\partial x} M_j \mathrm{d}x\mathrm{d}y, \tag{10}$$

$$\mathbf{C}_y^1(i,j) = \int\int_{\Omega^1} \frac{\partial N_i}{\mathrm{d}y} M_j \mathrm{d}x\mathrm{d}y, \tag{11}$$

where Ω^1 is the total area of the patch. The local stability condition can then by formally stated as follows.

Definition

A patch of elements is said to be *locally* stable if the patch pressure matrix has a rank of $m-1$.

In simple terms, the eigenvector corresponding to the only null singular value must be the constant vector, i.e. if $\mathbf{C}^1\mathbf{p}^1 = \mathbf{0}$ then $\mathbf{p}^1$ is constant.

The importance of being able to construct simple patches of elements which are locally stable is the fact that any grid which can be generated by grouping together stable patches will give an overall mixed approximation which is guaranteed to be stable is the sense that (5) is satisfied, with the constant c independent of h. This result is formally proved in Reference 12.

To illustrate the applicability of local stability theory, two simple elements are analysed. The first example considered is the uniformly stable element which was introduced above; the second example is a non-uniformly stable element which will be shown to have interesting local stability properties.

Example 1

Consider the general mixed approximation

$$V^h = \{(v_x^h, v_y^h): v_x^h|_{\Delta_k} = Q_c, v_y^h|_{\Delta_k} = Q_c \text{ for all } \Delta_k \in T_h\},$$

$$Q^h = \{q^h: q^h|_{\Delta_k} = L_c \text{ for all } \Delta_k \in T_h\}.$$

consider first an arbitrary patch of two elements as illustrated in Figure 1. The patch pressure matrix in this case is

$$\mathbf{C}^1 = \begin{bmatrix} \frac{1}{6}(y_q - y_r) & \frac{1}{6}(y_s - y_p) & \frac{1}{6}(y_p - y_s) & \frac{1}{6}(y_r - y_q) \\ \frac{1}{6}(x_r - x_q) & \frac{1}{6}(x_p - x_s) & \frac{1}{6}(x_s - x_p) & \frac{1}{6}(x_q - x_r) \end{bmatrix}. \tag{12}$$

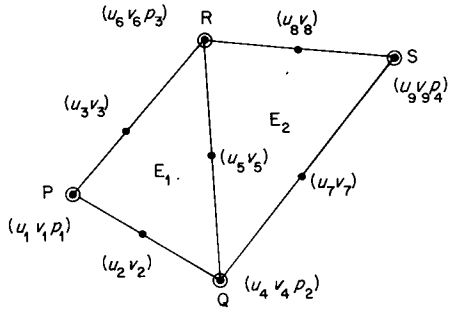

Figure 1. Degree of freedom for velocity (●); degree of freedom for pressure (○)

Assuming that nodes do not coincide, the matrix equation $\mathbf{C}^1\mathbf{p}^1 = \mathbf{0}$ implies that $p_2 = p_3$ and $p_1 = p_4$. In simple terms, the two pressures on the inter-element edge are equal, and the two pressures off the inter-element edge are equal. Obviously, two-element patches cannot be locally stable since there are four pressures and the rank of the patch pressure matrix is at most two.

Consider now arbitrary patches of three elements. There are two possibilities, which are illustrated in Figure 2. In either case, it is evident that the internal node conditions, that the pressures on inter-element edges are equal and the pressures off inter-element edges are equal, must imply that all the pressures over the patch are equal, i.e. $\mathbf{C}^1\mathbf{p}^1 = \mathbf{0}$ implies that $\mathbf{p}^1$ is constant, so all patches of three elements must be locally stable.

Considering larger patches, it can be proved by induction using the three-element patch that any patch consisting of more than three elements must also be locally stable. Finally, since all possible grids with more than two elements can always be decomposed into stable patches consisting of at most five elements, (5) is satisfied for any regular subdivision, so the element is uniformly stable.

Example 2

Consider the general approximation

$$V^h = \{(v_x^h, v_y^h): v_x^h|_{\Delta_k} = Q_c, v_y^h|_{\Delta_k} = Q_c \text{ for all } \Delta_k \in T_h\},$$
$$Q^h = \{q^h: q^h|_{\Delta_k} = L_d \text{ for all } \Delta_k \in T_h\},$$

i.e. continuous quadratic approximation of the two components of velocity with discontinuous linear approximation of the pressure corresponding to the three mid-side nodes. Although it has been pointed out previously, for example by Griffiths,[13] that this element can exhibit two spurious pressure modes, its stability properties do not appear to have been analysed before. Consider first the arbitrary patch of two elements as illustrated in Figure 3. The patch pressure matrix in this case is

$$\mathbf{C}^1 = \begin{bmatrix} \frac{1}{3}(y_q - y_p) & \frac{1}{3}(y_p - y_r) & 0 & \frac{1}{3}(y_s - y_q) & \frac{1}{3}(y_r - y_s) \\ \frac{1}{3}(x_p - x_q) & \frac{1}{3}(x_r - x_p) & 0 & \frac{1}{3}(x_q - x_s) & \frac{1}{3}(x_s - x_r) \end{bmatrix}$$

Clearly, the two-element patch cannot be locally stable since there are a total of five pressures and the rank of the patch pressure matrix is at most two. Also evident from the structure of the patch pressure matrix is the origin of the spurious chequerboard pressure modes, namely the zero coefficients corresponding to the pressure on the inter-element edge.

The propagation of the spurious pressure modes can be demonstrated by extending the two-

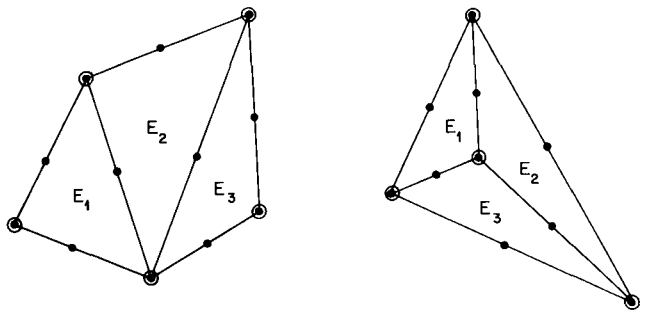

Figure 2. Degree of freedom for velocity (●); degree of freedom for pressure (○)

element patch to the three-element patch illustrated in Figure 4. The resulting pressure matrix will have two extra columns since there are two additional pressures, and two extra rows corresponding to the single additional internal node; thus the rank deficiency of the patch pressure matrix is still at least three. Using the same argument, it can be deduced that a locally stable patch can never be formed by appending an additional element to one of the edges of a smaller patch which is not locally stable. This is a fundamental difference between this element and the uniformly stable element in example 1.

The only way of generating locally stable patches from unstable patches in this case is to introduce additional elements which adjoin two edges of the original patch, so as to increase the number of rows in the patch pressure matrix without a similar increase in the number of columns. A simple example of a patch of elements which is locally stable is the patch of three isosceles triangles which is illustrated in Figure 5. The local stability can be established in this case by calculating the singular value decomposition of the corresponding patch pressure matrix.

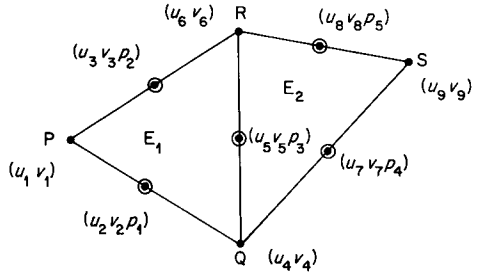

Figure 3. Degree of freedom for velocity (●); degree of freedom for pressure (○)

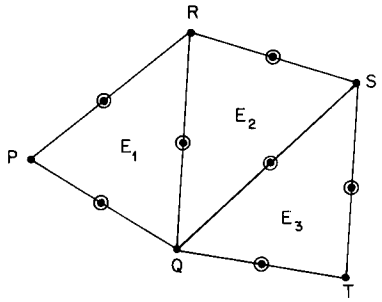

Figure 4. Degree of freedom for velocity (●); degree of freedom for pressure (○)

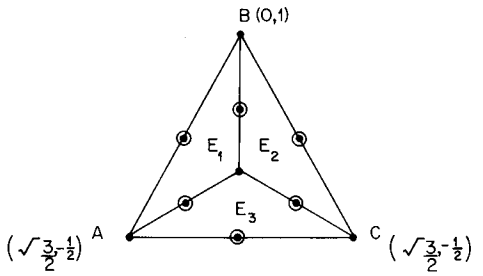

Figure 5. Degree of freedom for velocity (●); degree of freedom for pressure (○)

The intrinsic sensitivity of the element is perhaps best illustrated by studying the two patches of elements which are illustrated in Figures 6 and 7. Calculating the corresponding patch pressure matrices it is easily verified that the eight-element patch with the union-jack triangulation is locally stable, but that the patch with the unidirectional triangulation is not. In the unidirectional case the patch pressure matrix has a rank deficiency of three and the patch clearly exhibits the two spurious chequerboard pressure modes. This local stability behaviour has critical implications for the stability of mixed approximations in general, and in particular for the common case of a rectangular domain which is subdivided into a grid of equally sized elements by first dividing the domain into rectangles, and then subdividing each rectangle into two triangles. Applying local stability theory, it is known that if the triangulation algorithm generates a grid such that the elements can be grouped into stable eight-element patches, as is the case for the grids in Figure 8, then the resulting mixed approximation is guaranteed to be stable. On the other hand, if the triangulation strategy generates a grid of elements which cannot be grouped into stable eight-element patches, as is the case for the grids in Figure 9, then the stability of the mixed approximation is no longer guaranteed.

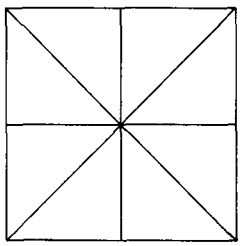

Figure 6.

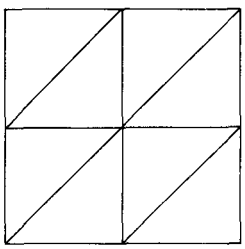

Figure 7.

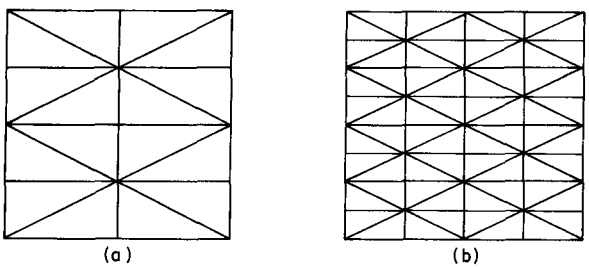

Figure 8. (a) grid GX1; (b) grid GX2

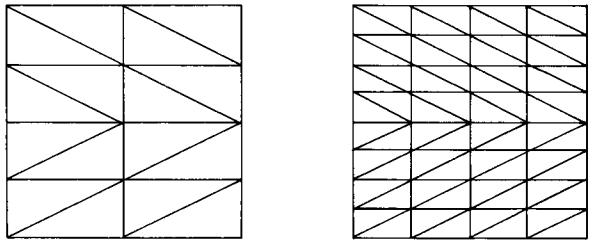

Figure 9. (a) grid G1; (b) grid G2

The dire consequences of using this element without guaranteed stability will be demonstrated in the following section.

NUMERICAL EXAMPLES

In order to investigate the relationship between the stability of the mixed approximations and the accuracy and rate of convergence of solution, a number of non-trivial flow problems were solved using the uniformly stable element and the semi-stable element analysed above. Results for two of the problems studied are presented here: for further details see Reference 14.

Example 1

The first example is the classical lid-driven cavity problem. Exploiting the symmetry, only half the domain was modelled ($0 \leqslant x \leqslant 0{\cdot}5; 0 \leqslant y \leqslant 1$); appropriate boundary conditions in this case are no flow on the fixed walls including the point ($x = 0, y = 1$), zero tangential velocity and zero normal stress on the symmetry boundary, with zero normal velocity and unit tangential velocity on the lid. No pressure specification is formally required since the hydrostatic pressure level is determined naturally by the normal stress condition.

In order to investigate the convergence properties of the elements used, two sequences of uniformly refined grids were generated. The first sequence of grids was generated from the initial grid G1, illustrated in Figure 9, by subdividing every element into four smaller elements while preserving the direction of the triangulation. The resulting grid G2 is also illustrated in Figure 9. Subsequent grids G3, G4 and G5 were generated in exactly the same way. A feature of all the grids in the sequence is the fact that they are all viable, for both of the elements analysed in the last section, in the sense that the global pressure matrices arising in the discretized systems of equations are of full rank, i.e. there are no 'pure' pressure modes. In the case of the semi-stable element, however, the grids are not guaranteed to give rise to stable mixed approximations, since the elements cannot be grouped into locally stable patches on any of the grids. The second sequence of grids was generated from the initial grid GX1, illustrated in Figure 8, by subdividing every rectangular two-element patch into a union-jack patch of eight elements. The generated grid GX2 is also illustrated in Figure 8. Subsequent grids GX3, GX4 and GX5 were generated in exactly the same way. The feature of all the grids in this second sequence is the fact that, using either of the elements analysed in the last section, the stability of the resulting mixed approximation is guaranteed.

Clearly, it is impossible to calculate the exact accuracy, and hence the order of convergence, of the numerical solutions when the problem being modelled does not have an analytic solution. However, it is possible to measure the exact pressure error in a restricted sense here, since it is

known that on the line of symmetry the pressure solution should be identically zero. Exploiting this fact, the following measure of the pressure error can be defined:

$$E = \left\{ \int_{\mathfrak{L}} p^2 \, ds \right\}^{1/2}. \tag{13}$$

By definition, numerical solutions are said to be converging with order α if the error E is proportional to h^α, where h is a measure of element length. For a sequence of uniformly refined grids, the order of convergence can be estimated from the solutions on successive grids by means of the formula

$$\alpha = \frac{\log [E(h)/E(h/2)]}{\log 2} \tag{14}$$

If the error in the solution cannot be calculated exactly, as is the case here for the velocity solution, then it is still possible to obtain an indication of the rate of convergence by monitoring the rate at which solutions approach each other with increased refinement of the grid.

A physically important measure of the global accuracy of the velocity solution for this problem is the position S of the stagnation point on the line of symmetry, since it is the centre of the primary recirculation. The three quantities E, the symmetry-line pressure error, α, the associated order of convergence of the pressure solution, and S, the position of the stagnation point, form the basis of the comparison here between the two elements that were analysed in the last section. The results for the uniformly stable element using the first sequence of grids for a Reynolds number of three are presented in Table I. Slightly esoteric behaviour using coarse grids is to be expected because of the influence of the pressure singularity at the point (0, 1). The effect of the singularity can be seen to diminish with increased grid refinement, as expected. The order of convergence estimates on the finest grids are clearly approaching the value of two which is optimal using linear approximation of the pressure. The tabulated values of S illustrate the rapid convergence of the velocity solution. Indeed, calculating the value of the quantity β given by

$$\beta = \frac{\log [S(h) - S(h/2)] - \log [S(h/2) - S(h/4)]}{\log 2} \tag{15}$$

using the values of S corresponding to grids G2, G3 and G4 gives a crude measure of the order of convergence of the velocity solutions of 3·09; by comparison, 3·00 is the optimal rate for quadratic approximation of the velocity.

Almost identical results to those in Table I were obtained with the uniformly stable element using the second sequence of grids; again both the pressure and the velocity could be seen to be converging at the optimal rates on the finest grids. The results obtained with the semi-stable element using the first sequence of grids are very different however. They are reproduced here in

Table I. Performance of the uniformly stable element using the first sequence of uniformly refined grids

Grid	E	α	S
G1	0·272		0·77586
G2	$0{\cdot}363 \times 10^{-1}$	2·91	0·76584
G3	$0{\cdot}291 \times 10^{-2}$	3·64	0·76512
G4	$0{\cdot}718 \times 10^{-3}$	2·02	0·76503
G5	$0{\cdot}173 \times 10^{-3}$	2·05	0·76503

Table II. These results vividly illustrate the disastrous consequences of not having the stability of the mixed approximations guaranteed. Far from converging at the optimal rate the pressure solution in this case can be seen to diverge, with an asymptotic rate of divergence of one on the finest grids. If the numerical solutions are analysed more closely it is obvious that the source of the errors in the pressure solutions is the singularity at the point (0, 1). Essentially, the pressure singularity seems to excite an 'impure' chequerboard pressure mode which persists over the entire grid. As illustrated by the tabulated pressure errors on the symmetry line, the magnitude of this impure pressure mode doubles with each successive uniform refinement of the grid. What is important to appreciate here is that the poor performance of this element is only manifest when the flow problem is 'difficult'; solving trivial problems using the same sequence of grids, ostensibly accurate pressure solutions can be obtained, since there are no 'pure' pressure modes. Similar behaviour is observed by Oden and Jacquotte,[7] and by Malkus and Olsen,[9] using semi-stable penalty finite element methods when the problem that is being solved is sufficiently 'difficult'.

A point of considerable importance is that whereas smoothing or filtering the pressure solution will effectively stop the growth of the pressure error, it does not affect the corresponding velocity solutions, and these are also unstable, as is evident from the values of the stagnation point position that are recorded in Table II. On the three coarsest grids the values appear to be converging to a *different* value to that calculated using the uniformly stable element, but the trend is not continued on the finest grids.

Using the semi-stable element such that the stability of the mixed approximation is guaranteed, i.e. using the second sequence of grids, gives the set of results in Table III. In this case the results closely resemble those of the uniformly stable element in Table I. Again, the pressure solution converges with the optimal rate on the finest grids; the value of β corresponding to the three finest grids suggests that the order of convergence of the velocity solutions is 3·00, and the calculated values of the stagnation point position agree to five decimal places on the finest grid.

Table II. Performance of the semi-stable element using the first sequence of uniformly refined grids

Grid	E	α	S
G1	3·29		0·76902
G2	4·33	−0·40	0·76408
G3	7·22	−0·74	0·76343
G4	13·3	−0·88	0·76349
G5	25·6	−0·94	0·76545

Table III. Performance of the semi-stable element using the second sequence of uniformly refined grids

Grid	E	α	S
GX1	1·43		0·74885
GX2	$0{\cdot}833 \times 10^{-1}$	4·10	0·76554
GX3	$0{\cdot}170 \times 10^{-1}$	2·29	0·76530
GX4	$0{\cdot}442 \times 10^{-2}$	1·94	0·76506
GX5	$0{\cdot}113 \times 10^{-2}$	1·97	0·76503

Example 2

The second example is that of flow through an expansion. The geometry and boundary conditions that were used are illustrated in Figure 10. As in the first example, two sequences of uniformly refined grids were generated. The first sequence was generated from the initial grid G1 illustrated in Figure 11, by subdividing every element into four, preserving the direction of the triangulation. The second sequence was generated from the initial grid GX1 illustrated in Figure 11, by subdividing into locally stable union-jack patches of eight elements. As in the first example, there are no 'pure' pressure modes using any of these grids using the boundary conditions of Figure 10. In the case of the semi-stable element, the stability of the mixed approximation is guaranteed for the second sequence of grids, but not for the first.

As expected, the pressure solutions using the semi-stable element without guaranteed stability were oscillatory; again the source of the oscillations was the singularity, i.e. the re-entrant corner at (4, 0·5). Unlike the driven cavity problem, however, the magnitude of the pressure oscillations did not grow in this case with increased grid refinement. To show this, the average pressures at the inlet $\bar{P}_i$ and outlet $\bar{P}_o$ for a Reynolds number of three were calculated using

$$\bar{P} = \frac{\int p \, ds}{\int ds}, \tag{16}$$

giving the results presented in Table IV. As in the driven cavity problem, the uniformly stable element can be seen to give consistently the most accurate pressures. In the case of the semi-stable

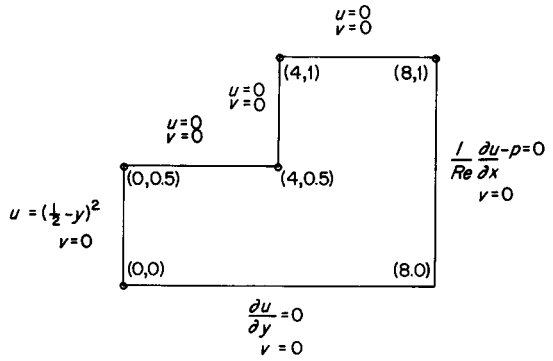

Figure 10.

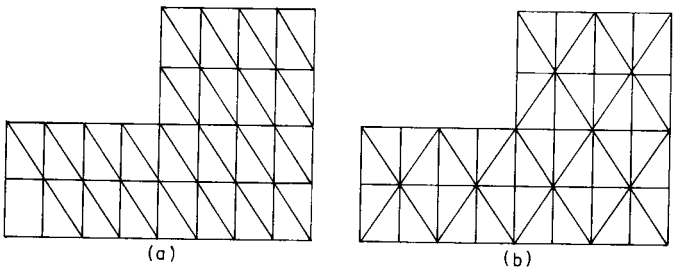

Figure 11. (a) grid G1; (b) grid GX1

Table IV. Comparison of average pressures at inlet and outlet

Stable element			Semi-stable element					
Grid	$\bar{P}_i$	$\bar{P}_o$	Grid	$\bar{P}_i$	$\bar{P}_o$	Grid	$\bar{P}_i$	$\bar{P}_o$
G1	3·194	0·000	G1	3·345	0·016	GX1	3·285	0·010
G2	3·182	0·000	G2	3·265	0·020	GX2	3·218	0·000
G3	3·176	0·000	G3	3·229	0·018	GX3	3·193	0·000
G4	3·174	0·000	G4	3·212	0·014	GX4	3·182	0·000
G5	3·173	0·000	G5	3·205	0·011	GX5	3·177	0·000

Table V. Comparison of the flow across the line $x = 6$

Stable element		Semi-stable element			
Grid	$\bar{u}$	Grid	$\bar{u}$	Grid	$\bar{u}$
G1	0·083044	G1	0·084171	GX1	0·081345
G2	0·083320	G2	0·083411	GX2	0·083230
G3	0·083333	G3	0·083320	GX3	0·083332
G4	0·083333	G4	0·083326	GX4	0·083333
G5	0·083333	G5	0·083331	GX5	0·083333

element, the pressure solutions are physically realistic only when the stability is guaranteed.

A feature of both the uniformly stable and the semi-stable elements is that in neither case is mass conserved over the element. In general, the semi-stable element is more incompressible than the uniformly stable one though, there being about three times the number of constraint equations. Far enough away from the singularity, the deleterious effect of using unstable mixed approximations on the incompressibility of the resulting velocity solution is particularly noticeable, e.g. calculating the 'volume' of flow $\bar{u}$ across the line $x = 6$ using the formula

$$\bar{u} = \int_0^1 u(6, y)\mathrm{d}y, \tag{17}$$

gives the results in Table V. The values can all be seen to be converging to the exact value of 0·083333, but the rate of convergence is significantly more rapid when the stability of the mixed approximation is guaranteed.

Using the position of the stagnation point as a measure of the rate of convergence of the velocity solution was not pursued, because the location of the stagnation point in this case is much closer to the singularity than in the driven cavity case. Consequently, the point velocities near the stagnation point were a long way from being converged; even the uniformly stable element results agreed only to about four decimal places on the two finest grids. Investigating the accuracy of the velocity solutions it is obvious that, as in the driven cavity case, the uniformly stable element point velocities are consistently more accurate than those of the semi-stable element. Comparing the relative accuracy of the semi-stable element point velocities, it is evident that the velocity solutions corresponding to grids giving guaranteed stability are almost everywhere *more* accurate than the solutions corresponding to grids without guaranteed stability; by way of illustration, the velocities at the point (5, 0·75) are compared in Table VI.

Table VI. Comparison of the velocities at the point (5, 0·75)

Stable element			Semi-stable element					
Grid	u	v	Grid	u	v	Grid	u	v
G1	0·04793	0·00377	G1	0·04272	0·00573	GX1	0·05107	0·00367
G2	0·05020	0·00266	G2	0·04971	0·00436	GX2	0·04997	0·00333
G3	0·05040	0·00263	G3	0·05002	0·00315	GX3	0·05012	0·00283
G4	0·05044	0·00260	G4	0·05022	0·00280	GX4	0·05028	0·00268
G5	0·05046	0·00259	G5	0·05034	0·00267	GX5	0·05038	0·00263

POSTSCRIPT

It is stressed that the results presented herein are indicative of a general phenomenon, namely that the accuracy of both velocities and pressures can be adversely affected by not having a scheme that is stable in a sufficiently strong sense. Other researchers have observed similar behaviour using non-uniformly stable quadrilateral elements. Further research is under way to analyse the stability of two-dimensional quadrilateral elements and, more importantly, three-dimensional brick elements, in more detail.

ACKNOWLEDGEMENT

The authors would like to acknowledge the assistance of Dr. M. Keech from the University of Manchester Regional Computer Centre's CYBER 205 unit in obtaining the computational results presented in the paper.

REFERENCES

1. I. Babüska, 'The finite element method with Lagrangian multipliers', *Numer. Math.*, **20,** 179–192 (1973).
2. F. Brezzi, 'On the existence, uniqueness and approximation of saddle point problems', *R.A.I.R.O. Analyse Numerique*, **8,** 129–151 (1974).
3. F. Thomasset, *Implementation of Finite Element Methods for Navier–Stokes Equations*, Springer Series in Computational Physics, Springer-Verlag, Berlin, 1981.
4. M. Fortin, 'Old and new finite elements for incompressible flow', *Int. j. numer. methods fluids*, **1,** 347–364 (1981).
5. R. Sani, P. Gresho, R. Lee, D. Griffiths and M. Engelman, 'The cause and cure (?) of the spurious pressures generated by certain FEM solutions of the incompressible Navier–Stokes equations', *Int. j. numer. methods fluids*, **1,** 17–43 (part I), 171–204 (Part II) (1981).
6. M. Engelman, R. Sani, P. Gresho and M. Bercovier, 'Consistent vs. reduced integration penalty methods for incompressible media using several old and new elements', *Int. j. numer. methods fluids*, **2,** 25–42 (1982).
7. J. Oden and O. P. Jacquotte, 'Stability of some mixed finite element methods for Stokesian flows', *Comp. Meths. Appl. Mech. Eng.*, **43,** 231–247 (1984).
8. C. Johnson and J. Pitkäranta, 'Analysis of mixed finite element methods related to reduced integration', *Math. Comp.*, **38,** 375–400 (1982).
9. D. Malkus and E. Olsen, 'Obtaining error estimates for optimally constrained incompressible finite elements', *Comp. Meths. Appl. Mech. Eng.*, **45,** 331–353 (1984).
10. V. Crouzeix and P. Raviart, 'Conforming and nonconforming finite element methods for solving the stationary Stokes equations', *R.A.I.R.O. Analyse Numerique*, **7,** 33–76 (1973).
11. M. Bercovier and O. Pironneau, 'Error estimates for finite element method solution of the Stokes problem in the primitive variables', *Numer. Math*, **33,** 211–224 (1979).
12. R. Stenberg, 'Analysis of mixed finite element methods for the Stokes problem: a unified approach', *Math. Comp*, **42,** 9–23 (1984).
13. D. Griffiths, 'The effect of pressure approximations on finite element calculations of incompressible flows', in *Numerical Methods for Fluid Dynamics*, Academic Press, London, 1982, pp. 359–374.
14. D. J. Silvester and R. W. Thatcher, 'A semi-stable mixed FE method for incompressible flow problems', *Numerical Analysis Report* 116, Manchester/UMIST Joint Series, 1986.